

## Video Article

# Laser-scanning Photostimulation of Optogenetically Targeted Forebrain Circuits

Charles C. Lee<sup>1</sup>, Ying-Wan Lam<sup>2</sup>, Kazuo Imaizumi<sup>1</sup>, S. Murray Sherman<sup>2</sup><sup>1</sup>Department of Comparative Biomedical Sciences, School of Veterinary Medicine, Louisiana State University<sup>2</sup>Department of Neurobiology, University of ChicagoCorrespondence to: Charles C. Lee at [clee@lsu.edu](mailto:clee@lsu.edu)URL: <http://www.jove.com/video/50915>DOI: [doi:10.3791/50915](https://doi.org/10.3791/50915)

Keywords: Neuroscience, Issue 82, optogenetics, cortex, thalamus, channelrhodopsin, photostimulation, auditory, visual, somatosensory

Date Published: 12/27/2013

Citation: Lee, C.C., Lam, Y.W., Imaizumi, K., Sherman, S.M. Laser-scanning Photostimulation of Optogenetically Targeted Forebrain Circuits. *J. Vis. Exp.* (82), e50915, doi:10.3791/50915 (2013).

## Abstract

The sensory forebrain is composed of intricately connected cell types, of which functional properties have yet to be fully elucidated. Understanding the interactions of these forebrain circuits has been aided recently by the development of optogenetic methods for light-mediated modulation of neuronal activity. Here, we describe a protocol for examining the functional organization of forebrain circuits *in vitro* using laser-scanning photostimulation of channelrhodopsin, expressed optogenetically via viral-mediated transfection. This approach also exploits the utility of cre-lox recombination in transgenic mice to target expression in specific neuronal cell types. Following transfection, neurons are physiologically recorded in slice preparations using whole-cell patch clamp to measure their evoked responses to laser-scanning photostimulation of channelrhodopsin expressing fibers. This approach enables an assessment of functional topography and synaptic properties. Morphological correlates can be obtained by imaging the neuroanatomical expression of channelrhodopsin expressing fibers using confocal microscopy of the live slice or post-fixed tissue. These methods enable functional investigations of forebrain circuits that expand upon more conventional approaches.

## Video Link

The video component of this article can be found at <http://www.jove.com/video/50915/>

## Introduction

The elaborate circuitry of the mammalian forebrain poses an experimental challenge to dissecting the functional roles of its intertwined components. Untangling these relationships has been aided recently by the development of optogenetic methods for specifically exciting and inhibiting neuronal populations and their projections<sup>1-3</sup>. These approaches make use of the genetically controlled expression of membrane channels responsive to light<sup>4-6</sup>. Of particular note, channelrhodopsin, a light-gated ion channel, depolarizes neuronal membranes following optical stimulation, leading to excitation of the expressing neuron and its projections<sup>4,7</sup>. Conversely, halorhodopsin, a light-gated chloride pump, hyperpolarizes the membrane, thus inhibiting the targeted projection<sup>6,8,9</sup>. Several variants of these opsins have been engineered, multiple vectors produced for transfection and expression in neuronal populations of interest, and transgenic mouse lines engineered that constitutively express these opsins or that enable cre-lox mediated control of their expression<sup>1,2,10,11</sup>.

The utility of these optogenetic methods and materials has revolutionized modern experimental neuroscience, enabling the dissection of the role of specific neural circuits in the physiology and behavior of the organism<sup>12-15</sup>. In particular, these methods can be powerfully applied to the functional dissection of brain circuits using *in vitro* slice preparations<sup>16-20</sup>. In this context, one of the main advantages of this method is the ability to characterize the physiology of long range projections that are difficult, if not impossible, to preserve in a thick slice, such as the commissural connections between cerebral cortical hemispheres<sup>16</sup>. Furthermore, this technology enables manipulations not possible with other methods, such as the selective inhibition of projections with fine temporal precision using halorhodopsin<sup>6,8,9</sup>. Moreover, the cell-type specific expression of these opsins allows isolated components in a neural circuit to be selectively stimulated or inhibited<sup>1,2,11,15,21</sup>. As such, these novel optogenetic tools enable the unprecedented analysis of the neuronal contributions to physiology and behavior.

Here, we describe a protocol for expressing channelrhodopsin in the mouse brain using adeno-associated viral (AAV) vectors<sup>1,2</sup>. Specific transfection of targeted neuronal populations can be accomplished using this protocol, with the appropriate choice of promoter constructs or transgenic mice that express Cre-recombinase in the targeted neurons of interest and a 'floxed' viral construct<sup>1,11,15,21</sup> (**Figure 1**). As examples here, we examine the corticocortical projections between the primary visual cortex (V1) and the secondary visual cortex (V2) and we also investigate the layer 6 corticothalamic projection from the primary somatosensory cortex (S1) to the ventroposterior medial nucleus (VPm). We combine this specific expression with laser-scanning photostimulation *in vitro* to assess synaptic physiology and functional topography. The

setup presented here enables the precise spatial positioning and control of the loci of photostimulation. Finally, we describe the visualization of expression patterns using confocal microscopy.

## Protocol

### 1. Surgery and Injections

1. Anesthetize mice using an intraperitoneal injection (22-25 G needle recommended) of ketamine (100-120 mg/kg) and xylazine (7.5-16 mg/kg).
  1. Assess sedation using strong toe pinches until no responses are elicited. For all animal procedures described, modify to follow local IACUC guidelines as necessary.
2. Place sedated mice in a stereotaxic device by securing the head and ears in their respective holders.
  1. Lubricate the eyes prior to placing the animal in the stereotaxic device with a sterile ophthalmic ointment.
3. Shave the scalp with a razor and sterilize the area with Betadine swabs.
4. Using a scalpel, cut a midline incision and reflect the skin and underlying muscles above the area to be injected.
5. Rotate a scalpel blade as a trephine to perform a craniotomy above the region to be exposed. Alternatively, use a small drill bit attached to a Dremel to perform the craniotomy.
  1. To perform the craniotomy, place scalpel blade or drill bit on surface of skull and slowly rotate until enough bone has been excavated to reveal the pia mater underneath.
  2. Once the initial excavation is made, enlarge the craniotomy using fine forceps to carefully remove bone from the edges.
6. Fill a 1  $\mu$ l syringe with the viral solution to be injected (UNC Vector Core).
  1. To enhance transfection efficacy, prepare viral solution with 4  $\mu$ g/ml polybrene.
7. Lower the needle into the area to be injected and pressure infuse 200 nl of solution containing virus with a syringe pump.
  1. Let syringe sit for 10 min before withdrawing the needle.
8. Suture the skin with nonabsorbable monofilament Nylon and cover the incision with antibiotic ointment.
  1. Sutures should be removed after 7-10 days.
9. Inject buprenorphine (0.05-0.1 mg/kg) for post-operative analgesia.
10. Allow animals to post-operatively recover for 14-21 days to allow for adequate expression of channel rhodopsin.

### 2. Slice Preparation

1. Following the recovery period, deeply anesthetize the animal with isoflurane anesthesia, as verified by absence of withdrawal reflex when the hind foot and/or toes are firmly pinched.
2. Dissect the brain by decapitation followed by midline and frontal cuts to the skull.
3. Peel apart the skull from the midline to expose the brain.
4. Carefully remove the brain using a fine scoop spatula to separate the cranial nerves from the base of the brain.
5. Quickly place dissected brain in small 100 ml beaker containing chilled, ice-cold artificial cerebrospinal fluid (ACSF; in mM: 125 NaCl, 3 KCl, 1.25  $\text{NaH}_2\text{PO}_4$ , 1  $\text{MgCl}_2$ , 2  $\text{CaCl}_2$ , 25  $\text{NaHCO}_3$ , 25 glucose).
6. Remove brain from ACSF and place on a microscope slide covered with filter paper prewetted with ACSF.
7. Make a blocking cut of the brain in the desired orientation using a clean razor blade.
8. Affix the blocked surface of the brain to cutting stage using instant adhesive glue.
9. Transfer stage to a vibratome cutting chamber (kept in freezer until ready for cutting).
10. Pour ice cold ACSF into cutting chamber.
11. Slice brain sections at 400-500  $\mu$ m using a vibrating tissue slicer.
12. Transfer brain slices to a holding chamber containing oxygenated ACSF, and incubate at 30 °C for at least 1 hr before experiment.

### 3. Physiological Recording

1. After the incubation period, transfer a slice to a recording chamber on a modified microscope stage.
2. Secure the slice in the bath during the experiment using a few threads of Nylon filaments attached to a platinum wire slice holder.
3. Perfuse the slice with ACSF constantly.
4. Pull recording pipettes to a tip resistance of 3-6 M $\Omega$  when filled with intracellular solution containing the following (in mM): 127 K-gluconate, 3 KCl, 1  $\text{MgCl}_2$ , 0.07  $\text{CaCl}_2$ , 10 HEPES, 2  $\text{Na}_2\text{-ATP}$ , 0.3  $\text{Na-GTP}$ , 0.1 EGTA. The intracellular solution should have pH 7.3, adjusted with KOH or gluconic acid and the osmolality of 280-290 mOsm.
5. Using a standard visualized whole-cell recording setup, place recording pipette near neuron to be recorded while applying positive pressure<sup>22,23</sup>.
6. Release positive pressure while applying suction to form Gigaohm seal.
7. Apply brief suction to break membrane and form whole-cell configuration recording.
8. Record the responses of neurons in either voltage or current clamp.

## 4. Laser-scanning Photostimulation

1. Start data acquisition software and hardware, described in previous reports<sup>23-29</sup>.

Note: We have utilized both Tidelwave<sup>25</sup> and, more recently, Ephus<sup>26</sup> acquisition programs, written in Matlab and developed by the laboratory of Karel Svoboda at Janelia Farms<sup>30</sup>. For a full description of laser-scanning photostimulation in Ephus, see Suter *et al.*<sup>26</sup> and the step-by-step guide<sup>30</sup>.

Note: The setup described in this article is derived from that described by Shepherd (2012)<sup>23</sup>. The laser beam is guided via an open beam system of mirrors to the top port of the microscope through the objective lens onto the slice (**Figure 2**).

2. Divert a small portion of the laser onto a photodiode with a microscope coverslip placed in the laser path and use the current output from this photodiode to monitor the laser intensity during experiments.
  1. Calibrate the photodiode current output recorded in the software to the measured laser power at the back focal plane of the objective using a power meter during equipment setup<sup>23</sup>.
3. Control the laser power by rotating a variable neutral density wheel. The laser power used varied between 25-70 mW (at the back focal plane) in our experiments.
4. Set the length and timing of the laser stimulating by modifying the pulse parameters for the laser and shutter. Laser stimulation is typically 2 msec long.
5. Capture image of the region to be stimulated using the 'Grab Video' function.
6. Select the stimulation grid according to desired dimensions. We typically use a 16 x 16 stimulation array with 80 µm spacing between adjacent rows and columns.
7. Overlay the mapping grid with the acquired image and adjust the x, y, and degree offset to the desired location and orientation.
8. Activate the 'Map' function to start stimulation and acquisition of data.
9. Following acquisition of photostimulation evoked responses, carry out analysis of mapped data using either the offline map analysis program in Tidelwave<sup>25</sup> or the 'MapAnalysis' program in Ephus<sup>26</sup>.

## 5. Fixed Slice Imaging

1. After recordings, transfer brain slice to 4% paraformaldehyde (PFA) in 0.01 M PBS (pH7.4) overnight at 4 °C.
2. Transfer the slice in 30% sucrose in 4% PFA/0.01 M PBS overnight at 4 °C.
3. Cut 50 µm sections using a cryostat and collect in 0.01 M PBS.
4. Rinse sections in 0.01 M PBS twice at room temperature.
5. Mount sections and coverslip in an appropriate antifade medium.
6. Transfer sections to the confocal microscope.
7. Focus into the ROI using white light.
8. Choose the wavelength, imaging size, and repetition for image acquisition. For YFP, we use 514 nm (Ex)/527 nm (Em).

## Representative Results

Laser-scanning photostimulation of projections between the primary visual area (V1) and the secondary visual area (V2) in the mouse was accomplished following injections of pAAV-CaMKIIa-hChR2(H134R)-EYFP into V1 of a Balb/C mouse (**Figure 3**). The CaMKIIa promoter in this viral construct drives specific expression of channelrhodopsin-EYFP in excitatory glutamatergic neurons<sup>1,15</sup>. After preparation of slices for physiological recording, expression of channelrhodopsin-EYFP fibers, *i.e.* epifluorescence of the conjugated EYFP, was observed traversing from V1 to V2 (**Figure 3A**). In addition, the corticothalamic fibers in the lateral geniculate nucleus (LGN) were also observed (**Figure 3A**). Whole-cell patch clamp recordings from a neuron in V2 revealed EPSCs elicited following laser-scanning photostimulation of channelrhodopsin-EYFP expressing fibers in the lower layers of V2 (**Figure 3B**).

In another example, laser-scanning photostimulation of the corticothalamic projections from layer 6 of the primary somatosensory cortex (S1) to the ventroposterior nucleus (VP) was accomplished using this protocol. Here, we used a Cre-Lox approach to specifically target channelrhodopsin expression in the layer 6 neurons and corticothalamic projections of interest. Explicitly, we injected pAAV-Ef1a-DIO-hChR2(H134R)-EYFP-WPRE-pA into S1 of B6.Cg-Tg(Ntsr1-cre)GN220Gsat/Mmcd mice (**Figures 1 and 4**). This transgenic mouse strain expresses Cre-recombinase specifically in layer 6 corticothalamic neurons<sup>21</sup>, and therefore results in ChR-YFP expression only in those neurons following transfection by the 'floxed' AAV construct. After preparation of slices, channelrhodopsin-EYFP fibers were observed in the layer 6 neurons and fibers projecting to layer 4 and VP (**Figures 4A and 4B**). Physiological recording from a VPm neuron using whole-cell patch clamp revealed that EPSCs could be elicited following laser-scanning photostimulation near the recorded neuron (**Figures 4C and 4D**).

The morphology of labeled fibers was assessed more readily following physiological recordings. Here, we resectioned (50 µm) slice preparations with channelrhodopsin-EYFP expression in layer 6 corticothalamic neurons (**Figure 5**). This revealed a fine pattern of labeled fibers traversing from layer 6 to layer 4, where they terminated and arborized extensively (**Figure 5A**). In addition, corticothalamic fibers were observed entering the white matter traversing towards the thalamus (**Figures 5A and 5B**).

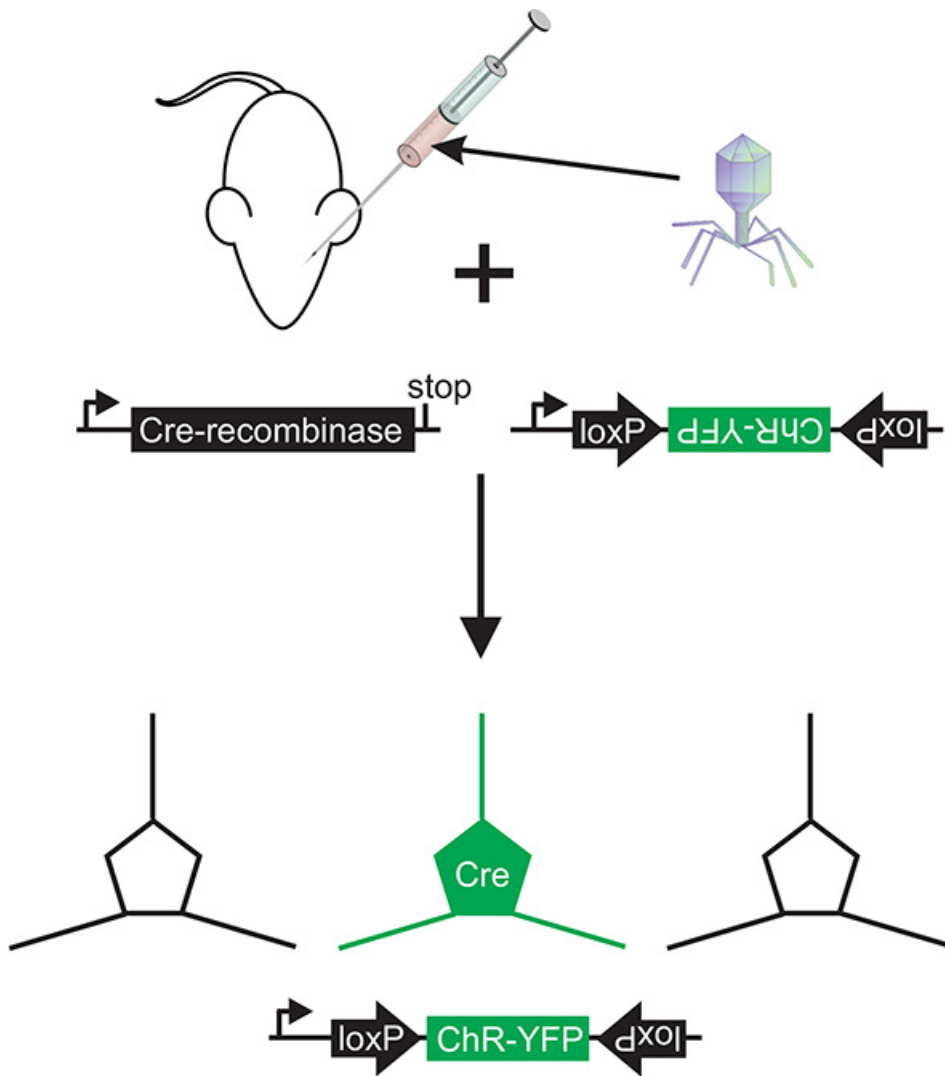


**Figure 1. Schematic illustration of targeted expression of channelrhodopsin via a Cre-Lox approach.** Transgenic mice expressing Cre-recombinase in the neuronal populations of interest are injected with a 'floxed' virus encoding channelrhodopsin fused to a fluorescent protein, such as YFP. Following transfection, only neurons with Cre-recombinase will express channelrhodopsin-EYFP. [Click here to view larger image.](#)

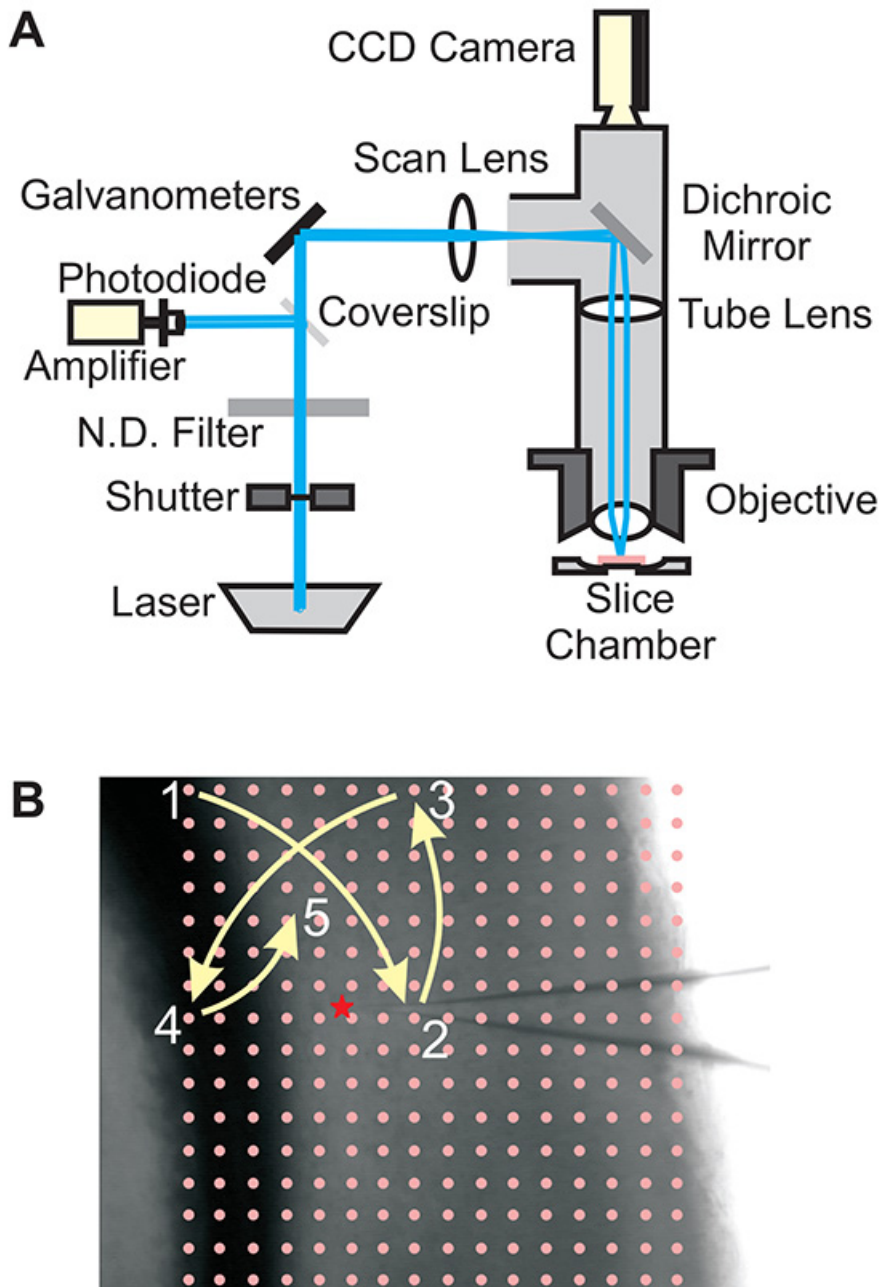


**Figure 2. Schematic illustration of photostimulation setup.** (A) Diagram of the laser-scanning photostimulation setup. The laser beam is guided successively through an open beam system to a shutter and a neutral density (N.D.) filter. A coverslip reflects part of the beam to a photodiode connected to an amplifier for laser power measurements. Mirror galvanometers are used to position the laser beam through a scan lens, which guides the beam through a side port on the top of the microscope. The beam is then reflected down through the objective lens to the slice preparation using a dichroic mirror. For further details see Lam and Sherman<sup>23</sup> and Shepherd<sup>29</sup>. (B) Example of the photostimulation grid pattern for the representative experiment shown in Figure 3. The 16 x 16 stimulation grid is overlaid on a photomicrograph of the slice preparation. A red star indicates the location of a neuron recorded using whole-cell patch clamp. The laser-beam position is guided to each of the 256 positions in the stimulation grid by computerized positioning of the mirror galvanometers. The laser positions of the 1st 5 stimulation sites are depicted in the figure. The responses from the recorded neuron to photostimulation at each of the sites is depicted in Figure 3. [Click here to view larger image.](#)

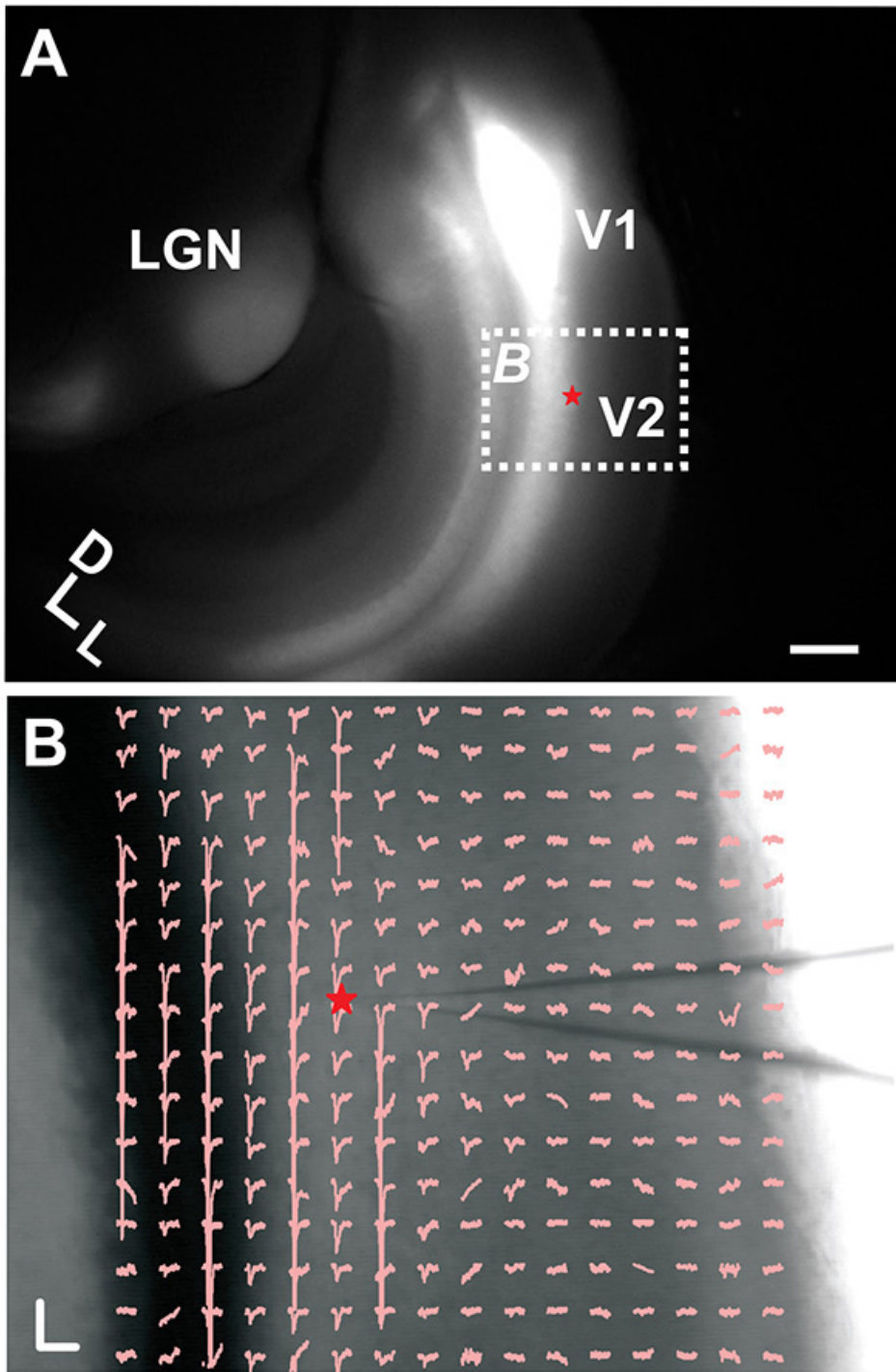


**Figure 3. Laser-scanning photostimulation of corticocortical projections from primary visual cortex (V1) to secondary visual cortex (V2) in the mouse.** (A) Epifluorescent image of the slice preparation showing channelrhodopsin-EYFP fibers from V1 to V2 and in the lateral geniculate nucleus (LGN). Specific expression of channelrhodopsin-EYFP in excitatory glutamatergic neurons is driven by a viral construct containing the CaMKIIa promoter. (B) Excitatory postsynaptic currents (EPSCs) elicited from a neuron in V2 following laser-scanning photostimulation. Red star indicates recording site. Scale bars: (A) 500  $\mu\text{m}$ , (B) 200 pA, 100 msec. [Click here to view larger image.](#)

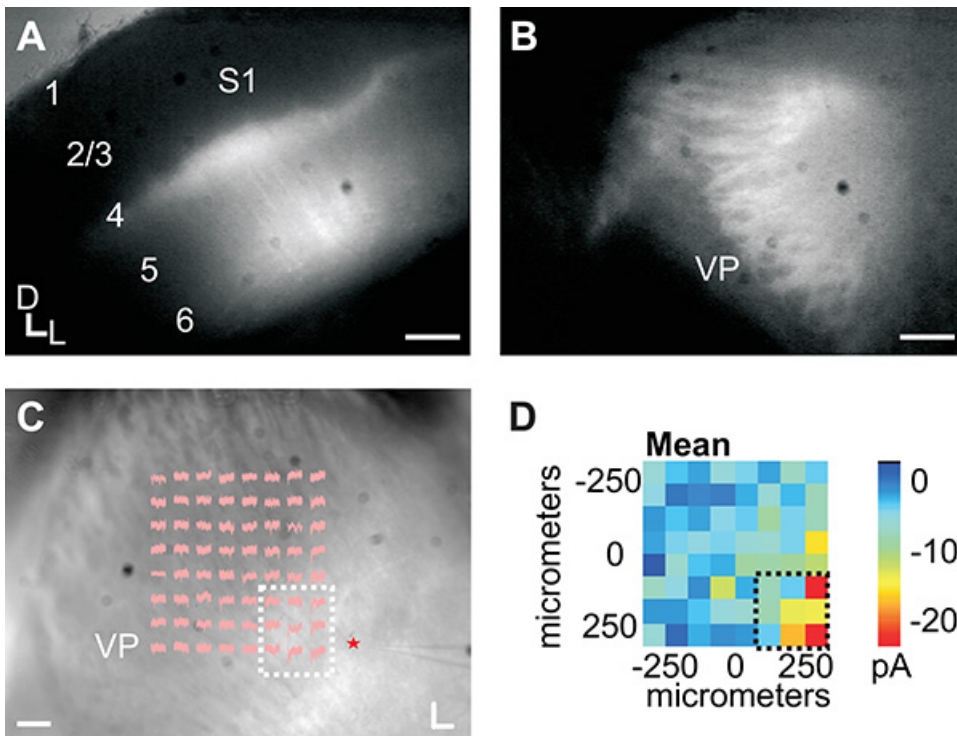


**Figure 4. Laser-scanning photostimulation of corticothalamic projections from primary somatosensory cortex (S1) to the ventroposterior nucleus (VP) in the mouse.** (A) Epifluorescent image of the slice preparation showing channelrhodopsin-EYFP fibers in S1. (B) Epifluorescent image of labeled-fibers in VP. (C) Excitatory postsynaptic currents (EPSCs) elicited from a VP neuron following laser-scanning photostimulation. (D) Plot of mean EPSCs. Red star indicates recording site. Boxed traces in (C) correspond with boxed values in (D). Scale bars: (A) 250  $\mu\text{m}$ , (B) 250  $\mu\text{m}$ , (C) 100 pA, 100 msec. [Click here to view larger image.](#)

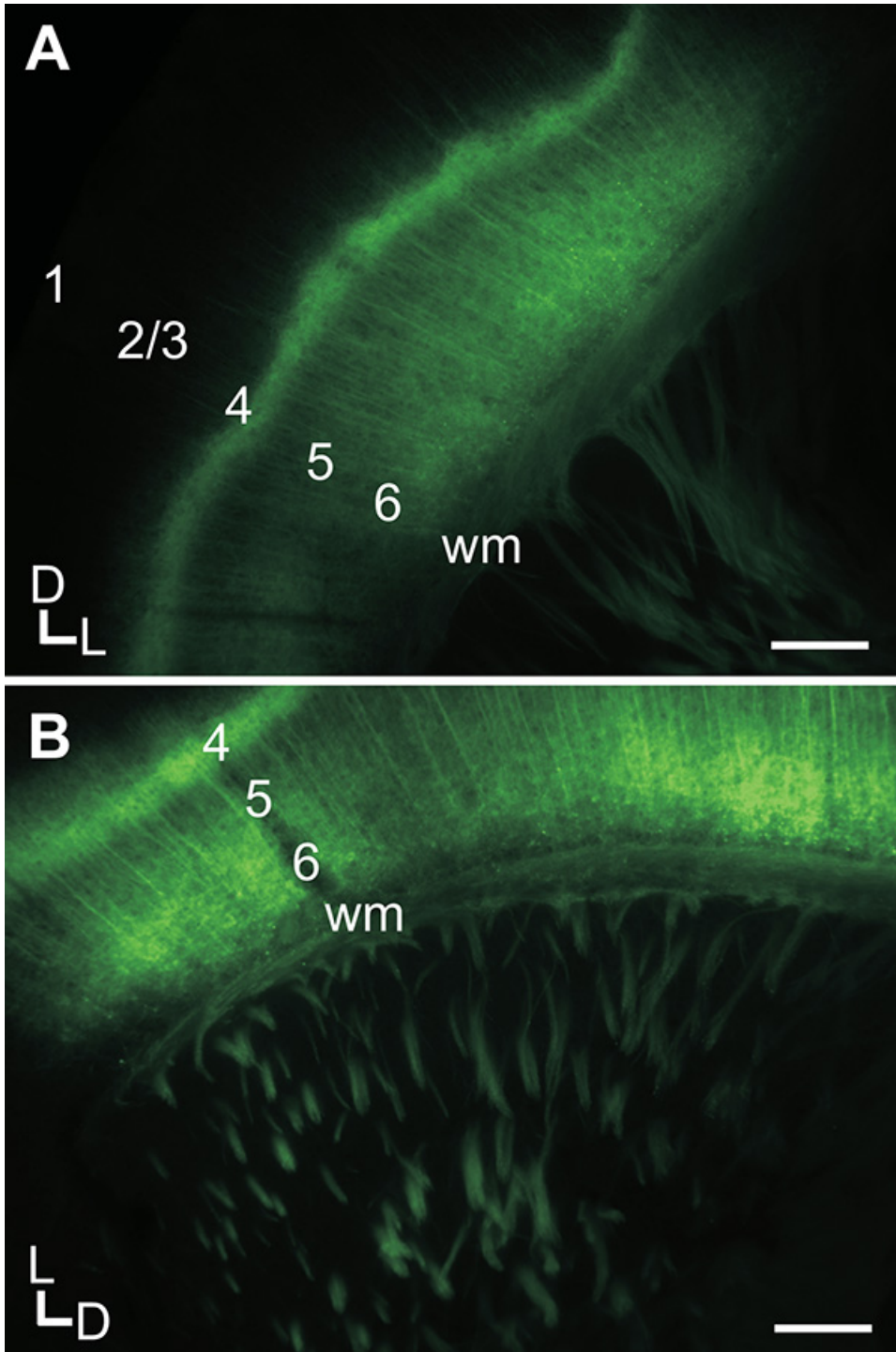


**Figure 5. Imaging of layer 6 neurons expressing channelrhodopsin-EYFP in the primary somatosensory cortex (S1) of the mouse. (A-B)** Labeled neurons in layer 6 and fibers projecting to layer 4 and the white matter. Scale bars: (A) 250  $\mu$ m, (B) 250  $\mu$ m. [Click here to view larger image.](#)

## Discussion

The described protocol details an approach for the *in vitro* assessment of functional topography and physiology of neuronal circuits, which is not limited to the investigation of forebrain circuits, *i.e.* those of the thalamus and cortex. Several viral constructs for optogenetic transfection have been made available to the scientific community and are readily obtainable from the UNC Vector Core. For a description of viral constructs readily available, see the UNC Vector Core<sup>31</sup>, the optogenetics resource page at the Deisseroth Lab at Stanford University<sup>32</sup> and the Boyden synthetic neurobiology lab at MIT<sup>33</sup>. Variants of these opsins have been developed by these labs and enable wide-ranging modes for controlling



neuronal excitability<sup>1,2</sup>. Obtaining these vectors from the UNC Vector Core requires a Material Transfer Agreement from the originating labs. In this protocol, we note that the addition of polybrene enhances transfection efficacy. In addition, another variable influencing expression is the post-surgical recovery period, which we note that a period of at least 14 days is sufficient to obtain robust expression in the forebrain pathways of mice.

For the targeted transfection of specific neuronal groups, several Cre-transgenic mouse lines have been developed, which can be used in combination with 'floxed' reversed open reading frame viral constructs that have been developed<sup>11</sup>. Several strains pertinent to neuroscience research are available through the Mutant Mouse Regional Resource Centers<sup>34</sup>. Atlases of Cre-recombinase expression patterns in these transgenic lines are offered through the GENSAT database<sup>35</sup>. In addition, Jackson Labs offers several Cre-transgenic strains, as well as others that constitutively express opsins in specific neuronal groups. A critical step to utilizing these mouse lines is to factor in the time necessary for obtaining and establishing a breeding colony, which may vary based on the particular strain of interest.

For photostimulation, we have utilized and adapted the setup developed by the Shepherd Lab at Northwestern University, described in a recent protocol<sup>29</sup>. Although optimized for glutamate uncaging, this setup is amenable also for photostimulation of channelrhodopsin without modification. This setup enables precise spatial control and positioning of the loci of photostimulation, which enables an assessment of the functional topography of channelrhodopsin innervation of recorded neurons. Although spatial control is enhanced with this method of photostimulation, it is more cost prohibitive than methods utilizing LED based field illumination<sup>20</sup>. In addition, the nonuniformity of brain tissue is a limitation of optogenetics, or any techniques involving manipulation of light. In practice though, it is rarely a factor since results are interpreted mostly in a qualitative manner. In case more quantitative comparison between brain regions is needed, one can always use maximum light intensity to achieve "saturated" responses.

In addition, we have used both Tidelwave and Ephus software programs written in Matlab for controlling the laser-scanning photostimulation and data acquisition<sup>25,26</sup>. However, it is recommended that those setting up a similar system employ the newer Ephus software<sup>26</sup>, which has support available through the Janelia Farms development site<sup>30</sup>. A key step is choosing which of these software packages to use, since their hardware requirements differ slightly. In addition, the map analysis programs are tailored to their respective data acquisition programs.

Several of these steps can be modified to suit the practitioner's particular setup. Injections of viral solutions can be performed with delivery mechanisms besides a syringe, e.g. capillary glass pipettes pulled to tip diameters of ~40  $\mu\text{m}$  also work well. For surgeries, a nonstereotaxic headholder can be substituted if such coordinates are not required for guiding injections. In addition, ACSF and intracellular solution compositions may be altered depending on the particular experimental requirements, e.g. substituting a cesium or high chloride intracellular solution to isolate inhibitory currents. Also, an alternative to imaging of expression patterns in fixed slices may also be done in the live slice on a suitable imaging rig with a bath perfusion system.

In summary, this protocol will enable the practitioner to characterize the functional topography and synaptic physiology of projections *in vitro*, which may not be possible using standard methods, e.g. characterizing long-range projections that are unable to be preserved in a slice. The transfection protocol described can be applied to *in vivo* optogenetic experiments<sup>1-3,12,14</sup>, since the delivery mechanism is the same. Finally, although this protocol describes transfection of mice, many of the viral vectors available can be used to theoretically transfect and express these opsins in a wide range of mammalian species, thus enabling a myriad of comparative and species-specific studies<sup>1-3</sup>.

## Disclosures

The authors declare they have no competing interests. The author (CCL) received a publication grant from Leica Microsystems, which produces an instrument used in this filming of this protocol.

## Acknowledgements

This work was supported by NIH/NIDCD grant R03 DC 011361, SVM CORP grant LAV3202, NSF-LA EPSCoR grant PFUND86, and a publication grant from Leica Microsystems (CCL) and NIH/NIDCD grant R01 DC 008794 (SMS).

## References

1. Tye, K. M. & Deisseroth, K. Optogenetic investigation of neural circuits underlying brain disease in animal models. *Nat. Rev. Neurosci.* **13**, 251-266 (2012).
2. Bernstein, J. G. & Boyden, E. S. Optogenetic tools for analyzing the neural circuits of behavior. *Trends Cog. Sci.* **15**, 592-600 (2011).
3. Yizhar, O., Fenno, L. E., Davidson, T. J., Mogri, M. & Deisseroth, K. Optogenetics in neural systems. *Neuron*. **71**, 9-34 (2011).
4. Nagel, G. *et al.* Channelrhodopsin-2, a directly light-gated cation-selective membrane channel. *Proc. Natl. Acad. Sci. U.S.A.* **100**, 13940-13945 (2003).
5. Zemelman, B. V., Lee, G. A., Ng, M. & Miesenböck, G. Selective photostimulation of genetically ChARGed neurons. *Neuron*. **33**, 15-22 (2001).
6. Gradinaru, V., Thompson, K. R. & Deisseroth, K. eNpHR: a Natronomonas halorhodopsin enhanced for optogenetic applications. *Brain Cell Biol.* **36**, 129-139 (2008).
7. Boyden, E. S., Zhang, F., Bamberg, E., Nagel, G. & Deisseroth, K. Millisecond-timescale, genetically targeted optical control of neural activity. *Nat. Neurosci.* **8**, 1263-1268 (2005).
8. Lanyi, J. K. Halorhodopsin: A light-driven chloride ion pump. *Ann. Rev. Biophys. Biophys. Chem.* **15**, 11-28 (1986).

9. Han, X. & Boyden, E. S. Multiple-color optical activation, silencing, and desynchronization of neural activity, with single-spike temporal resolution. *PLoS One*. **2**, e299 (2007).
10. Zhao, S. *et al.* Cell type-specific channelrhodopsin-2 transgenic mice for optogenetic dissection of neural circuitry function. *Nat. Methods*. **8**, 745-755 (2011).
11. Madisen, L. *et al.* A toolbox of Cre-dependent optogenetic transgenic mice for light-induced activation and silencing. *Nat. Neurosci.* **15**, 793-802 (2012).
12. Fenno, L., Yizhar, O. & Deisseroth, K. The development and application of optogenetics. *Annu. Rev. Neurosci.* **34**, 389-412 (2011).
13. Gradinaru, V., Mogri, M., Thompson, K. R., Henderson, J. M. & Deisseroth, K. Optical deconstruction of parkinsonian neural circuit. *Science*. **324**, 354-359 (2009).
14. Olsen, S. R., Bortone, D. S., Adesnik, H. & Scanziani, M. Gain control by layer six in cortical circuits of vision. *Nature*. **483**, 47-52 (2012).
15. Zhang, F. *et al.* Optogenetic interrogation of neural circuits: technology for probing mammalian brain structures. *Nat. Protoc.* **5**, 439-456 (2010).
16. Petreanu, L., Huber, D., Sobczyk, A. & Svoboda, K. Channelrhodopsin-2-assisted circuit mapping of long-range callosal projections. *Na. Neurosci.* **10**, 663-668 (2007).
17. Cruikshank, S. J., Urabe, H., Nurmikko, A. V. & Connors, B. W. Pathway-specific feedforward circuits between thalamus and neocortex revealed by selective optical stimulation of axons. *Neuron*. **65**, 230-245 (2010).
18. Lee, C. C., Lam, Y. W. & Sherman, S. M. Intracortical convergence of layer 6 neurons. *Neuroreport*. **23**, 736-740 (2012).
19. Mancuso, J. J. *et al.* Optogenetic probing of functional brain circuitry. *Exp. Physiol.* **96**, 26-33 (2011).
20. Valley, M., Wagner, S., Gallarda, B. W. & Lledo, P. Using affordable LED arrays for photo-stimulation of neurons. *J. Vis. Exp.* (57), e3379, doi:10.3791/3379 (2011).
21. Gong, S. *et al.* Targeting Cre recombinase to specific neuron populations with bacterial artificial chromosome constructs. *J. Neurosci.* **27**, 9817-9823 (2007).
22. Cox, C. L. & Sherman, S. M. Control of dendritic outputs of inhibitory interneurons in the lateral geniculate nucleus. *Neuron*. **27**, 597-610 (2000).
23. Lam, Y. W. & Sherman, S. M. Mapping by laser photostimulation of connections between the thalamic reticular and ventral posterior lateral nuclei in the rat. *J. Neurophysiol.* **94**, 2472-2483 (2005).
24. Lam, Y. W. & Sherman, S. M. Functional organization of the somatosensory cortical layer 6 feedback to the thalamus. *Cereb Cortex*, **20**, 13-24 (2010).
25. Shepherd, G. M., Pologruto, T. A. & Svoboda, K. Circuit analysis of experience-dependent plasticity in the developing rat barrel cortex. *Neuron*. **38**, 277-289 (2003).
26. Suter, B. A. *et al.* Ephus: multipurpose data acquisition software for neuroscience experiments. *Front Neural Circuits*. **4**, 100 (2010).
27. Lee, C. C. & Sherman, S. M. Topography and physiology of ascending streams in the auditory tectothalamic pathway. *Proc. Natl. Acad. Sci. U.S.A.* **107**, 372-377 (2010).
28. Lee, C. C. & Sherman, S. M. Intrinsic modulators of auditory thalamocortical transmission. *Hear Res.* **287**, 43-50 (2012).
29. Shepherd, G. M. Circuit mapping by ultraviolet uncaging of glutamate. *Cold Spring Harb. Protoc.* **2012**, 998-1004 (2012).
30. ScanImage, Ephus, and other DAQ software [Internet]. Ashburn (VA): Janelia Farms. Available from: <http://www.ephus.org> cited May 9 (2003).
31. UNC Gene Therapy Center [Internet]. Chapel Hill (NC): University of North Carolina. Available from: <http://genetherapy.unc.edu/services.htm> cited May 9 (2003).
32. Optogenetics Resource Center [Internet]. Stanford (CA): Stanford University. Available from: <http://www.stanford.edu/group/dlab/optogenetics> cited May 9 (2003).
33. Synthetic Neurobiology Group [Internet]. Cambridge (MA); MIT. Available from: <http://syntheticneurobiology.org> cited May 9 (2003).
34. Mutant Mouse Regional Resource Centers [Internet]. Bethesda (MD): NIH. Available from: <http://www.mmrc.org> cited May 9 (2003).
35. GENSAT Brain Atlas [Internet]. Bethesda (MD): NIH. Available from: <http://www.gensat.org/cre.jsp> cited May 9 (2003).